A Comparison of the Properties of Selected Commercially Available, Low-cost Carbon Dioxide and Methane Gas Concentration Sensors

Wesley T. Honeycutt, Nicholas F. Materer, M. Tyler Ley

***Abstract*—This paper examines the suitability of commercially available, low-cost carbon dioxide and methane gas concentration sensors for use in a field deployable solar-powered monitoring devices. Sensors were selected based on market availability, cost, power consumption, detection range and accuracy. The precision and detection limits of each were determined using a gas mixing chamber coupled with a precision bench-top analyzer to characterize the sensor exposed to a known gas concentrations. For environmental monitoring, the selected carbon dioxide sensors were characterized around 400 ppm. For the methane, sensor response was monitored at 0 ppm, then gas concentrations were measured between 2 and 200 ppm. For both gases, exertions up to several 1000 pm were examined to mimic a leak. For sensors with significant power consumption, the turn-on time was quantified.**

***Index Terms*—Chemical sensors, Gas industry, Pollution measurement, Spectroscopy, Carbon, Chemistry, Gas detectors, Sensor systems and applications**

I. Introduction

ENVIRONMENTAL monitoring of local gas concentration is becoming increasingly important to ensure worker safety and for early identification of potential leaks. Real time monitoring of carbon dioxide and methane gas concentrations are of interest since these gases impact animal health and crop growth. Since gases are considered greenhouse gases, monitoring industrial sites are important in understand their impact on the environment. In designing monitoring devices, the sensor for gas concentration analysis must be matched to the specific operational requirements, such as precision, reliability, and power consumption. Example sensor elements include those used in HVAC air handlers [1], [2], chemical processing units [3], oil well monitoring devices [4], [5], and environmental monitoring [6]–[10]. Given the myriad of other applications, the uses cited represent only a small sample of the various applications and varieties of sensor elements. Despite the large number of sensors which are commercially available, there is limited literature that directly compares sensors. This lack of information limits ones ability to select the optimal sensor for a given application. To address this issue, this paper compares an array of commercially available, low-cost sensors for carbon dioxide (chemical formula CO_2) and methane (chemical formula CH_4) at concentration typical to those required for environmental monitoring around carbon dioxide sequestering operations and oil fields.

Potential sensors range from small, inexpensive chemiresistive sensors to complex and costly optical systems. The low-cost chemiresistive based methane sensors are typically used in gas warning systems [11]. On the other end, Light Imaging Detection and Ranging (LIDAR) is an accurate and effective method for remote monitoring of industrial sites, for example oil wells [12]. However, these devices are limited by cost and operational complexity, and are not suitable for portable self-powered monitoring devices. The sensors need good sensitivity and precision around the baseline atmospheric concentration for each analyte, which is around 400 ppm for carbon dioxide [13], [14] For methane, the baseline atmospheric concentration is under 2 ppm [15]–[17]. Thus, for methane, sensors were selected and tested near their baseline. In addition to concentration, power consumption, reliability, and ease of integration are also important factors. Sensors will be selected based on their sensitivity at atmospheric levels, ease of use, power consumption, price, and market availability.

II. Objectives

The objective of this study is to determine the suitability of commercially available low-cost sensors for integration into portable self-powered monitoring equipment. The low-cost sensors currently available can be generally divided by detection method, either optical absorption or electrical changes due to a chemical reaction with the analyte (chemiresistive). Previous researchers have cited concerns with electrochemical sensors for these gases, as they have a short lifetime and lack robustness [18]. Therefore, the selection process is focused on sensors that are commercially available in large volumes (at least 1000 units) at low-cost (defined here as less than $100 per unit in bulk).

Optical sensors typically have excellent stability, selectivity, and fast response to concentration changes. Optical methods of detecting carbon dioxide and methane are based on the measuring the absorption of light at $2352\,\mathrm{cm}^{-1}$ and $3015\,\mathrm{cm}^{-1}$, respectively [19], [20]. Sensors utilizing these specific wavelengths are termed dispersive infrared instruments and are typically costly, bulky, and delicate. Low-cost sensors utilize nondispersive infrared (NDIR) sensing, which utilizes a source

Department of Chemistry

W. Honeycutt and N. Materer are with the Department of Chemistry, Oklahoma State University, Stillwater, OK 74078 USA (e-mail: materer@okstate.edu).

T. Ley is with the Department of Civil Engineering, Oklahoma State University, Stillwater, OK 74078 USA (e-mail: tyler.ley@okstate.edu)

Research was funded in part by a grant from the U.S. Department of Energy.

Manuscript received MONTH XX, 2016; revised MONTH YY, 2016

Digital Object Identifier: 10.somenumber

which emits at a broad spectrum coupled with a narrow band pass filter across the absorbance maximum. As a result, lower cost parts can be used and the design can be both more compact and robust. These optical methods utilize the Beer-Lambert Law to relate absorptions to concentrations, and thus are only dependent on the geometry of the sensor and physical properties of the gas. [21] In general, NDIR detection is utilized for carbon dioxide do due its relatively large molar adsorption coefficient results in a short path length. Methane is limited in practical applications due to its low absorbance coefficient and overlap interfered symmetric C-H stretches, making methane difficult to distinguish from ethane or propane, for example. [22].

Chemoresistive sensors for carbon dioxide and methane are primarily based on reactions between the analyte and a semiconductor metal oxide film. Although, chemiresistive sensors have significant drawbacks, including selectivity, these sensors are easy to produce and have very low cost, leading to widespread use. Unlike optical sensors which depend only on physical properties of the analyte, the output of these sensors has a complex relationship to the gas concentration which varies from sensor to sensor. For carbon dioxide, the concentrations is based on resistance changes that occur when carbon dioxide adsorbs and reacts to form a carbonate on the surface of the film [23]. Given the availably and performance of NDIR sensors for carbon dioxide, this work did not evaluate chemiresistive sensor for this analyte. Commercially, there are several available chemiresistive sensors for detection of methane, typically tin oxide [18]. These sensors work by measuring changes in electron transport through the metal oxide semi-conductive film, in the presence of oxygen and reactive gases [24]. When the film is exposed to methane, the molecule adsorbs and reacts with surface oxygen species. This liberates free electrons in the bulk and reduces the electrical resistance [25], [26]. Since the measurement depends on the presence of oxygen containing species, the output depends on the relative humidity, temperature, and preparation of the film. For remote sensing, these sensors require between $300\,\mathrm{mW}$ and $600\,\mathrm{mW}$ of power to heat the metal oxide film to between $200\,^{\circ}\mathrm{C}$ and $450\,^{\circ}\mathrm{C}$ [27], which drastically increases power consumption and must be considered when designing a self-powered sensor platform.

III. Methods

To test the sensors under controlled conditions, a gas mixing apparatus (Fig. 1) was constructed. This setup allows gas flow of a known concentration to be prepared from a calibrated gas cylinder. A high-quality bench-top analyzer (California Analytical Instruments, Inc. ZRE Non-Dispersive Infrared Analyzer) sensitive to both carbon dioxide and methane. The analyzer can be periodically calibrated using the calibrated gas mixture to ensure accuracy. The calibrated gas tank contained a mixture of gases in one of the ratios listed in Table III depending on the specific experiment being performed. The gas mixtures were provided by and certified to these concentrations within $\pm 2\%$ of the declared value by Airgas Inc. The calibrated gas mixture diluted using either air or nitrogen gas by a set of flow controls to produce specific partial pressures of analyte

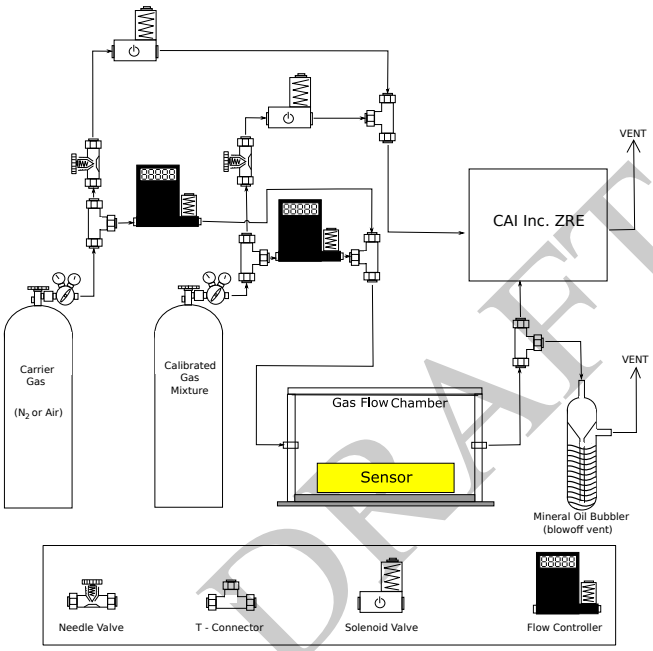

Fig. 1. Component diagram of controlled gas exposure apparatus with chamber for diffusion-type sensors.

gases. In the case of sensors configured for gas flow, the sensor being tested was connected directly to the apparatus by flexible hose connection. For sensors that are diffusion based, the sensor was placed in an exposure chamber connected by flexible hose. Using the exposure chamber, the relative rise time of the various sensors was measured and compared. The mixing time or the time required for the chamber to reach and maintain gas concentration, even when the concentration of the incoming gas was changing was determined to be negligible with respect to the response times of the sensors. All experiments were referenced to the California Analytical Instruments ZRE Analyzer.

Commercially available carbon dioxide and methane sensors were selected and evaluated based on the needs for a portable self-powered monitoring device. Table I lists the selected carbon dioxide sensors with important properties obtained from the manufacturer. Table II lists the methane sensors and respective properties. The K-30, COZIR, Dynament, and Telaire sensors are all NDIR sensors. These sensors were chosen as low-cost, lightweight sensors with satisfactory detection parameters of carbon dioxide. Dynament also provides a dual gas NDIR sensor designed to measure both carbon dioxide and methane concentrations. This ability was attractive given low-cost and portability requirements. The carbon dioxide and methane Gascard sensors sold by GHG Analytical were an order of magnitude more expensive than the other chosen NDIR sensors, which have a cost between that of the lowest cost sensors on our list and that of the bench-top analyzers. Their specifications combined with the included pressure and temperatures compensation make them attractive enough to make up for the expense. In addition to the Gascard sensor, the Dynament hydrocarbon sensors were chosen as the inexpensive candidates for methane detection. Chemoresistive sensors include the MQ-

TABLE I
MANUFACTURER LISTED PROPERTIES OF EVALUATED CARBON DIOXIDE SENSORS

Sensor	Supplier	Type	Sampling Method	Cal. Range	Op. Range
K-30 SE-0018	CO_2Meter	NDIR	flow or diffusion	0-5000 ppm	0-10000 ppm
COZIR AMB GC-020	CO_2Meter	NDIR	flow or diffusion	0-5000 ppm	0-10000 ppm
Gascard CO_2	GHG Analytical	NDIR	flow	0-50000 ppm	0-50000 ppm
MSH-P/CO2/NC/5/V/P/F	Dynament	NDIR	diffusion	0-2491 ppm	0-5000 ppm
MSH-DP/HC/CO2/NC/P/F	Dynament	NDIR	diffusion	100-2500 ppm	0-5000 ppm
Telaire T6615	General Electric	NDIR	flow or diffusion	0-2000 ppm	0-2000 ppm

Sensor	Warm Up	T	Humidity	Auto-cal	V Input	Avg. I
K-30 SE-0018	<1 min	0-50°C	0-95%	Yes	4.5-14 VDC	40 mA
COZIR AMB GC-020	<3 s	0-50°C	0-95%	Yes	3.25-5.5 VDC	1.5 mA
Gascard CO_2	30 s	0-45°C	0-95%	Yes	7-30 VDC	250 mA
MSH-P/CO2/NC/5/V/P/F	45 s	-20-50°C	0-95%	No	3.0-5.0 VDC	75-85 mA
MSH-DP/HC/CO2/NC/P/F	45 s	-20-50°C	0-95%	No	3.0-5.0 VDC	75-85 mA
Telaire T6615	10 min	0-50°C	0-95%	Yes	0-5 VDC	33 mA

TABLE II
MANUFACTURER LISTED PROPERTIES OF EVALUATED METHANE SENSORS

Sensor	Supplier	Type	Sampling Method	Cal. Range	Op. Range
MQ-4	Futurelec	Chemoresistive	diffusion		200-10000 ppm
Gascard CH_4	GHG Analytical	NDIR	flow	0-50000 ppm	0-50000 ppm
MSH-P/HC/NC/5/V/P/F	Dynament	NDIR	diffusion	0-5000 ppm	0-10000 ppm
MSH-DP/HC/CO2/NC/P/F	Dynament	NDIR	diffusion	5000-11000 ppm	0-10000 ppm
TGS-2600	Figaro Engineering	Chemoresistive	diffusion		1-30 ppm
TGS-2610	Figaro Engineering	Chemoresistive	diffusion		1000-25000 ppm
TGS-2611	Figaro Engineering	Chemoresistive	diffusion		500-10000 ppm

Sensor	Warm Up	T	Humidity	Auto-cal	V Input	Avg. I
MQ-4				No	5 VDC	<150 mA
Gascard CH_4	30 s	0-45°C	0-95%	Yes	7-30 VDC	250 mA
MSH-P/HC/NC/5/V/P/F	30 s	-20-50°C	0-95%	No	3.0-5.0 VDC	75-85 mA
MSH-DP/HC/CO2/NC/P/F	30 s	-20-50°C	0-95%	No	3.0-5.0 VDC	75-85 mA
TGS-2600				No	5.0±0.2 VDC	4.2±4 mA
TGS-2610				No	5.0±0.2 VDC	5.6±5 mA
TGS-2611				No	5.0±0.2 VDC	5.6±5 mA

Sensors with no listed warm up time, but required 7 day burn in time

TABLE III
RATIOS OF CALIBRATED GASES USED IN MIXED GAS EXPERIMENTS.

Carbon Dioxide	Methane	Carrier Gas
3000 ppm	3000 ppm	nitrogen
100 ppm	100 ppm	nitrogen
0 ppm	20 ppm	nitrogen

4 from Hanwei Electronics and TGS-2600, TGS-2610, and TGS-2611 manufactured by Figaro Engineering Inc. sensors. The TGS sensors are used in commercial methane detectors and have been previously evaluated by other groups [28]. There are several different MQ versions optimized for hydrocarbon sensing. The MQ-4 sensor was chosen as this variant was specifically tuned for methane. The chemiresistive sensors required various minimum conditioning periods before use by their respective manufacturers. This "burn-in" time was met or exceeded for all chemiresistive sensors.

A. Data Collection and Sensor Response Time

Due to the unique interface requirements of each sensor, development kits were purchased when possible. For those without development kits available, an Arduino microcontroller with a prototyping board was used. The chemiresistive sensors were energized using the recommend voltage for the heater element and the response was measured as voltage, after buffering and filtering, across a reference resistor (a 10 kΩ resistor was used for R_{ref}) in this experiment) [29]. This voltage ($V_{measured}$) can be converted to resistance (R) and conductivity (G) of the sensor element by the following:

$$R = \frac{V_{cc} - V_{measured}}{V_{measured} \times R_{ref}}$$

$$G = \frac{1}{R}$$

.

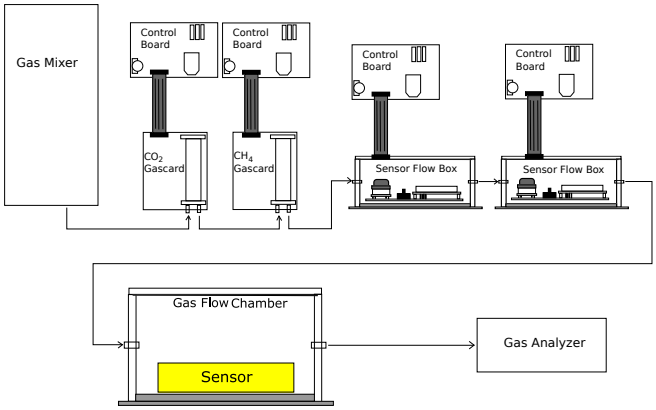

Fig. 2. The diagram shows the flow of gas from the mixing apparatus to Gascard sensors, small enclosures containing sensors, the large gas flow chamber, and finally to the California Analytical Instruments, Inc. ZRE Non-Dispersive Infrared Analyzer. The gas mixing apparatus is shown in Fig. 1.

The response of each sensor was logged as a function of time using software provided by the manufacturer as part of development kits when provided, or using an Arduino microcontroller with microSD card.

The baseline stability and sensor noise measurements were performed for each sensor using calibrated gas flow generated from the gas mixing apparatus as depicted in Fig. 1. Multiple sensors were in operated concurrently as shown in Fig. 2. The sensors are organized by flow capable sensors such as the Gascard units and environmental exposure-based sensors housed within the gas enclosures. Sensor modules in the small gas flow enclosures included the K30 carbon dioxide sensor and socket for chemiresistive methane sensors (MQ-4 and the TGS series). The larger chamber contained the COZIR, Telaire, Dynament, and K30 sensors. Given the large total volume, data collected from the sensors in this chamber were analyzed only after the system reached a constant concentration following the introduction a gas with known concentration of carbon dioxide or methane.

For the optical sensors, the sampling time was controlled by internal electronics, which sample several times a minute. For environmental monitoring application, the response from all sensors, with the only expectation of the chemiresistive sensors, were effectively immediate. Chemiresistive sensors responded on a notably different timescale that the optical sensors due to the thermal heating of the sensing element. In addition, the power requirement may require in these sensors to be periodically turned on and off. To address the response time of the chemiresistive sensors, the MQ-4 methane sensor was selected as a worst-case model sensor. For flow-through sensors, the response time can be measured with minimal delay due to the small system volume. For the chemiresistive sensor, the large volume utilized for the baseline and noise studies was not suitable for measuring the response time. To accurately measure the response for chemiresistive based sensor, a smaller sensor enclosure (internal volume $2.54\,\mathrm{cm}^3$) was constructed minimize the time to reach a stable new concentration.

B. Precision and Baseline Noise Tests

The measurement precision of each sensor was performed using the exposure apparatus discussed in Fig. 1. The baseline carbon dioxide tests were performed with a measured concentration of approximately 400 ppm in nitrogen gas, while the baseline methane tests were performed under medical grade air. The 0 ppm methane concentration was chosen as the expected atmospheric or environmental level will be less than 1 ppm [15], [17]. Medical grade air was utilized since the chemiresistive sensors required atmospheric concentrations of oxygen to correctly measure the methane concentration. The gas concentrations were verified with the bench-top analyzer (California Analytical Instruments, Inc. ZRE Non-Dispersive Infrared Analyzer). The precision of the sensors was determined by a 20 to 30-hour data collection run at a known concentration and uniform flow.

C. Sensor Calibration and Limit of Detection

Calibration curve of each sensor was established by varying concentrations of gas through system and, when appropriate, subtracting the baseline reading to the average concentration after stabilization. For a typical calibration curve, the carrier gas was first introduced. After a stable baseline was obtained, the calibrated concentration was introduced, after 24 hours, the calibrated gas was introduced, and after 24 hours, it was turned off. The carrier gas was reintroduced and the system was allowed to stabilize for the next measurement. During this procedure, contraction data from each sensor was continually collected. With this method, the average baseline and response to each concentration can be extracted. This process allows any inherent delay caused by the gas exchange in the system when the carrier gas was introduced into the system to be removed from the data stream before analysis. Any initial overshoot and ringing, as observed for the chemiresistive sensor were also edited from the data. The California Analytical Instruments Inc. ZRE Non-Dispersive Infrared Analyzer was used to verify the concentrations at each point on the calibration curves. The instrument was calibrated using gas supplied by Airgas Inc. within the 2% precision.

The collected data were analyzed by first performing a baseline correction, if required, at each carbon dioxide and methane concentrations. Both the mean (μ) and standard deviation (σ) were calculated from each individual baseline and average at each calibration point. The $\mu_{ZRE,peak}$ was the average response of the California Analytical Instruments Inc. ZRE. Thus, the plot of the calibration is as follows:

$$x = \mu_{ZRE,peak}$$
$$y = \mu_{sensor,peak} - \mu_{sensor,baseline}$$

.

The Limit of Detection (L_D) was then calculated for each sensor from the σ of the respected dataset using the standard approach [30], [31]:

$$L_D = 3 \times \sigma$$

Consistent with the Beer-Lambert law, the optical absorption based sensors all showed a linear response. Linear regression

was utilized to determine the calibration and standard error. The chemiresistive sensors produce non-linear calibration curves. Data sheets from the MQ-4 and TGS sensors showed significant non-linearity at low concentrations. The response curve was modeled using a Langmuir-like or Langmuirian form, which provided a response consistent with that specified by the manufacturer. Although forms have been suggested by kinetic analysis [32], [33], a Langmurian form provided the simplest fit. The following equation was utilized:

$$f(x) = \frac{a \times b \times x}{1 + b \times x}$$

Where a and b are undetermined constants. These were determined by fitting the experimental data using the Levenberg-Marquardt algorithm in $gnuplot$ [34].

The slope (m) and intercept (b) are used in calculations from the results of linear regression modeling for optical sensors, and the coefficients of the Langmuir isotherm (a) and (b) are used in calculations from the results of fitting the isotherm model. The mean of the calculated limit of detection of several individual trials (μ_{L_D}) was adjusted for each sensor. Since detection limits are not comparable across arbitrary and unrelated units, these values were correlated to the California Analytical Instruments Inc. ZRE Non-Dispersive Infrared Analyzer response by the calibration curve produced in the trendline. For optical sensors with a linear calibration curve:

$$LoD_{corr} = m \times LoD + b$$

For sensors fit to a Langmurian curve:

$$L_{D(corr)} = \frac{a \times b \times L_D}{1 + b \times L_D}$$

IV. Results and Discussion

A. Data Collection and Sensor Response Time

To provide an example of the data collected from the sensors, Fig. 3 shows the response of two selected carbon dioxide sensors, the K30 and Gascard, to 600 and 1400 concentration steps of carbon dioxide. These steps are just above and below the OSHA standard of 1000 ppm. The K30 reports the concentration directly, while the Gascard reports a value between zero and one, with one being the maximum concentration (3% carbon dioxide for the sensor purchased). Both optical sensors respond very quickly to an increase in carbon dioxide inside the environmental chamber. The data demonstrate relative similarity in behavior of the selected sensors in the presence of concentration changes well above the limit of detection.

Fig. 4 shows the response of the MQ-4 and TGS-2611 sensors, both optimized for methane detection, to a 100 and 1000 ppm concentration step of methane. The higher limit is the maximum National Institute for Occupational Safety and Health's (NIOSH) recommended safe methane concentration. The lower limit is more representative of a leak. The TGS-2611 sensors had a much faster and more step-like response to changes in methane concentration than the MQ-4 sensors. Similar behavior was also observed for a decrease in concentration. The magnitude of response is larger and noise, quantified next, is smaller for the TGS-2611 sensor.

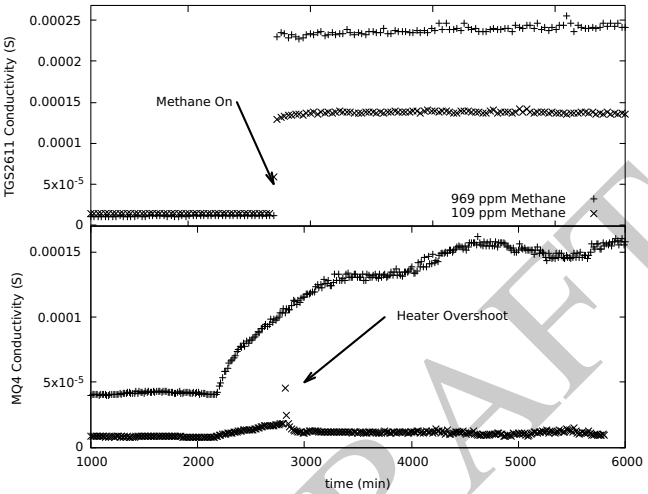

Fig. 3. The Gascard (top) and K30 (bottom) sensor response over time at high (1433 ppm, plotted with "×" on the plot) and low (577 ppm, plotted with "+" on the plot) concentrations of carbon dioxide.

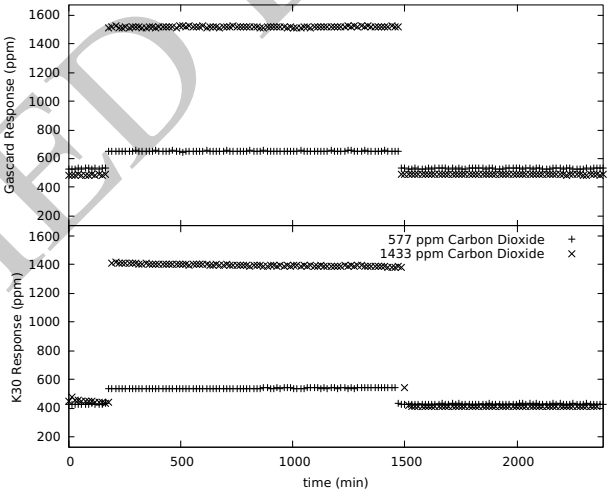

Fig. 4. Plots of the TGS-2611 (top) and MQ-4 (bottom) sensor response over time at high (969 ppm, plotted with "×" on the plot) and low (100 ppm, plotted with "+" on the plot) concentrations of methane.

Experiments were performed with a smaller sensor enclosure (internal volume 2.54 cm^3) for the MQ-4. As discussed in the Methods (section III), chemiresistive sensors responded on a different timescale than that of the optical sensors due to their internal heater. This internal heater also results in additional power requirements, possibly requiring these sensors to be periodically turned on and off for self-powered environmental sensing applications. Fig. 5 depicts a plot of the time response of an MQ-4 to changing concentrations.

The sensor produces a large, sharp overshoot, often exceeding 100% of the final response. Normally, sensors are characterized by rise time, the time for the response to change from 10% of the mean response to 90% of the mean response. These overshoots are likely a result of a complex set of chemical reactions and differing rates occurring at the

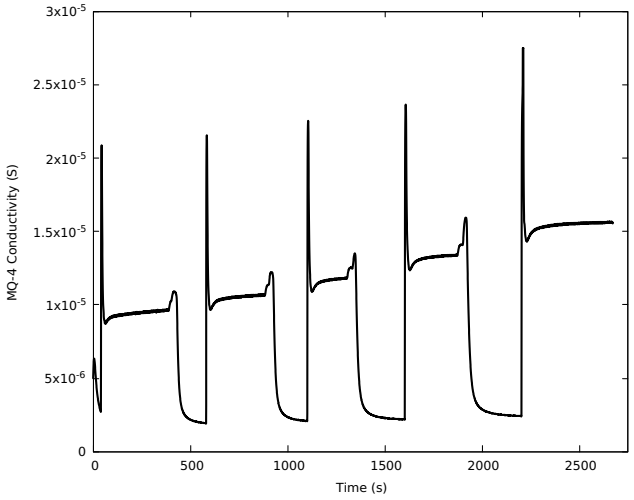

Fig. 5. The MQ-4 sensor showed noticeable delay between introduction of gas and production of a stable response. In this plot, the large overshoot during sensor cycling, likely caused by gas introduction into the mixing apparatus, is apparent.

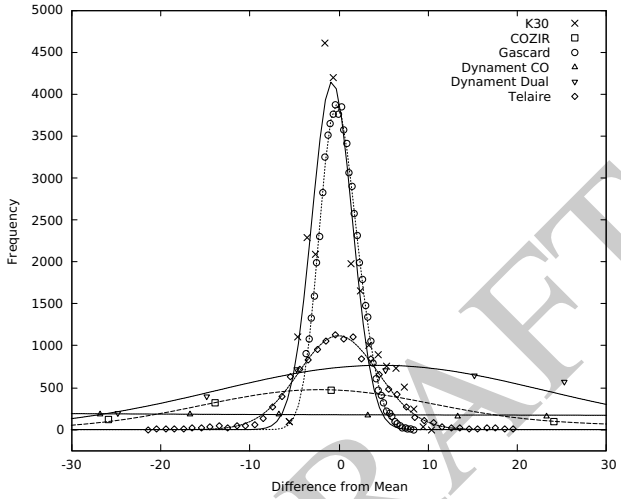

Fig. 6. Gaussian non-linear fitting results for the frequency distribution of fluctuations of each sensor around a baseline for the carbon dioxide sensors (see text).

surface. Given the large overshoot, the rise time is less useful for this system. Settling time, the time required to reach a steady state value after a concentration change, is more useful. The settling time for the MQ-4 sensor did not appear to be concentration dependent. A stable value was produced within 2.5% of the mean after $78\pm10\,\mathrm{s}$, averaged over all response time experiments. Similar response times are expected for the TGS sensors due to the similar sensing methods.

B. Precision and Baseline Noise Tests

The measurement precision of each sensor was performed as described in the Methods (section III). In most cases, the precision of the sensors was determined by a 20 to 30 hour data collection time at a known concentration under uniform flow. An initial Fourier analysis showed no significant periodic variations in the output during respective tests. Thus, distribution of the digitized sensor output around the mean was utilized. The data streams were processed to provide the individual difference from the mean reported value, and a histogram of these differences was plotted. The digitized sensor outputs have a finite number of possible output values, so no further bins were created while producing the analysis. A Gaussian fit was applied to the histograms to determine the degree of fit. The histograms, along with a best-fit Gaussian peak, can be seen in Figs. 6 and 7 for the carbon dioxide and methane sensors, respectively. The fit for the Dynament Dual sensor was not included, as this sensor only reported two values at the given concentration. The resolution of this sensor was not precise enough to determine the fluctuations. In addition, the fit for the MQ-4 curve is also not included in this plot. The MQ-4 distribution is very large and its range is several orders of magnitude larger than that found for the other sensors.

Sensor drift, or reported changes at constant concentration,was measured using the difference between the highest and lowest points in an extended run. A summary of results

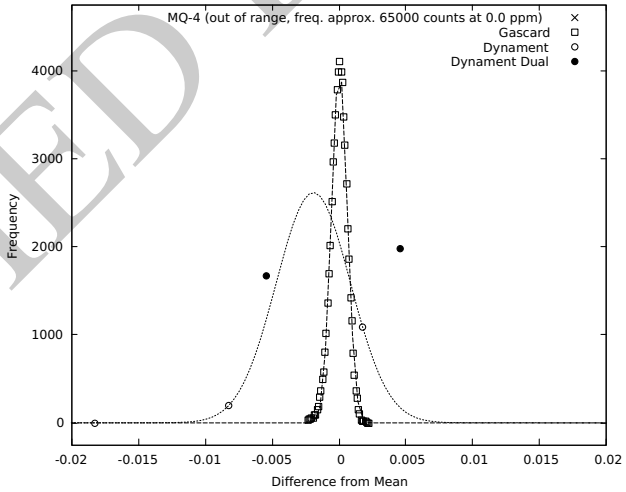

Fig. 7. Gaussian non-linear fitting results for the frequency distribution of fluctuations of each sensor around a baseline for methane sensors (see text).

from this analysis can be found in Tables IV and V. Statistical analysis data for these curves are reported in terms of standard deviation and the full width at half max (FWHM).

Of the carbon dioxide sensors show in Table IV, the Gascard and K-30 sensors both showed low noise given the relatively narrow distributions of response. The noise distribution from the Gascard sensor was Gaussian, having a FWHM of 5.01 ppm. The K-30 response was skewed toward higher concentration values and appears to show two overlapping peaks. These peaks have similar FWHM values, suggesting a shift in the mean measured value. Concentration in ppm values, being the ratio volume of the analyte to a unit volume, are dependent on temperature and pressure. It is possible that periodic temperature and pressure variations, which are corrected for by the Gascard sensor, are responsible for this skew. In general, precise work requires incorporation of pressure and temperature sensors into potential environmental sensing units to allow ppm corrections to be performed. The breadth of underlying

Gaussian peaks in the histogram of responses from the K-30 sensor suggests a similarly narrow distribution around the mean as the Gascard. For both of these sensors, the drift was ± 20 ppm.

The distribution of responses around the mean by the GE Telaire sensor produces a diffuse broad distribution compared to the relatively narrow on from the K-30 and Gascard sensors. The breadth of the GE Telaire peak (FWHM 10.4) is when compared to the K-30 sensor, as the sensing mechanism and path lengths are very similar. In the investigation of this phenomenon, it was experimentally discovered that the Telaire sensor is sensitive to ambient light levels.

Comparing the response for both the Telaire and K-30 sensors was monitored with and without ambient light. The data showed that the Telaire sensor is sensitive to ambient light sources. In a similar experiment with the K-30 sensor, the change in response from the K-30 sensor was negligible.

Of the methane sensors shown in Table V the Edinburgh Gascard normal distribution of responses around the reported mean from the Gascard is a very narrow peak, indicating a highest degree of precision. At times, the Gascard did report some relatively large fluctuations, several standard deviations around the mean response. Although these fluctuations could be explained by the exposed nature of the sensor during these tests, it suggests that some minimal digital filtering may be required when implementation into devices. The single gas Dynament methane sensor produced a narrow distribution of responses, but the results from the dual-gas Dynament sensor were inconclusive. The dual-gas Dynament sensor only reported two values for methane,around the mean rather than a normal distribution of several values. Approximating the FWHM by the difference between these two points around a mean, the dual-gas sensor would have a FWHM equivalent to that produced by the single-gas sensor. This indicates possible resolution issues dcause by the digitization of the response, and not fundamental issues with the sensor design. This assumption makes sense, as the Dynament sensors are optimized for hazard sensing, not for the precision required for environmental monitoring. Finally, the MQ-4 sensor produced a wide range of values. The distribution around the mean is so broad, that the tails are off the scale in Fig. 7. While the FWHM of these responses from the MQ-4 show that the peak only deviates 1.19 ppm around the mean, it is comparatively much less precise than the other sensors in the experiment.

For accuracy, all of the sensors must be calibrated before use, rather than used directly from the supplier. With the exception of the carbon dioxide and methane Gascard sensors, there was poor accuracy without an initial calibration. The Gascard, K-30, Telaire, COZIR, and Dynament carbon dioxide sensors, could be easily recalibrated by the sensor architecture. For portable self-powered units, the background level of carbon dioxide provides reasonable reference. In the more electronically simple chemiresistive sensors, periodic calibration is absolutely required for accuracy. Given that the response also depends strongly on temperature and humidity, use in precision instruments is unlikely. For devices such as the MQ-4 methane sensor, the expectation of good accuracy with time may be outside of reasonable expectation. However, for applications in which high concentration level changes (greater than 10 ppm) from the background concentration is expected, chemiresistive sensors are effective and low-cost.

TABLE IV
PRECISION AND ACCURACY OF CARBON DIOXIDE SENSORS

Sensor	σ	FWHM
K-30 SE-0018	1.91	4.51
COZIR AMB GC-020	14.1	33.3
Gascard CO_2	2.12	5.01
MSH-P/HC/CO2/	86.4	204
MSH-DP/CO2/	17.6	41.4
Telaire T6615	4.42	10.4

TABLE V
PRECISION AND ACCURACY OF METHANE SENSORS

Sensor	σ	FWHM
MQ-4[†]	0.507	1.19
Gascard CH_4	0.580	1.37
MSH-P/HC/CO2/	3.54	8.33
MSH-DP/HC/	no data	no data

[†] Data for the MQ-4 are listed in terms of electrical response rather than parts-per notation.
[‡] All data in Table IV is in units of ppm, while all data in Table V are in units of ppb.

C. Sensor Calibration and Limit of Detection

The sensor calibration and a limit of detection were determined as discussed in the Methods (section III). An example calibration plot with linear and non-linear trendlines is shown in Fig. 8. The correlated limits of detection are listed in Table VI. Of the tested carbon dioxide sensors, the Edinburgh Gascard shows the greatest sensitivity. This is consistent with expectations based on the path length of the sensor. The Dynament single analyte sensor shows a lower limit of detection than the dual analyte sensor produced by the same manufacturer. The K-30 and Telaire sensors show comparable detection limits. The COZIR sensor exhibits the poorest limit of detection.

Of the tested methane sensors, the Edinburgh Gascard again shows the greatest sensitivity. The MQ-4 and TGS2611 sensors, have very low limits of detection. It was observed that these thin film sensors were very sensitive to changes in temperature and humidity. It should be noted that these tests were carried out in a controlled environment which sought to eliminate those sources of error. An application without these sorts of controls may be subject to much more error. Furthermore, individual MQ-4 sensors varied a great deal in response compared to other sensors of the same type. The Dynament sensors have appear to have a limit of detection under 10 ppm. These

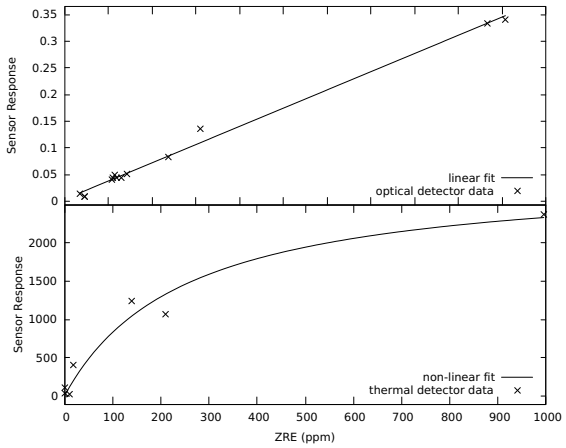

Fig. 8. A sample plot of the calibration of sensor signals to the California Analytical Instruments Inc. ZRE Non-Dispersive Infrared Analyzer reported concentration during carbon dioxide and methane spikes. The top part of the figure shows the response of an optical carbon dioxide sensor with the expected linear behavior. The bottom part of the figure shows the response of a chemiresistive methane sensor with a fit of the non-linear response.

TABLE VI
DETECTION LIMITS OF CARBON DIOXIDE SENSORS

	$L_{D(corr)}$
K-30 SE-0018	31.1
COZIR AMB GC-020	65.7
Gascard CO_2	0.00862
MSH-P/HC/CO2/	57.6
MSH-DP/CO2/	6.60
Telaire T6615	22.9

TABLE VII
DETECTION LIMITS OF METHANE SENSORS

	$L_{D(corr)}$
MQ-4	1.24†
Gascard CH_4	0.569
MSH-P/HC/CO2/	7.44‡
MSH-DP/HC/	2.42‡
TGS-2600	33.3†
TGS-2610	29.0†
TGS-2611	3.95†

† Calculated from Langmuirian fitting.
‡ Failed to produce consistent response within tested range.

numbers are artificially deflated. The Dynament sensors could not reliably detect any concentration of gas below 100 ppm, and these null results have skewed the trendline of detection limits. Values we observed cannot be guaranteed below this threshold. In Table VI, these datapoints are denoted with a double dagger (‡). The TGS-2600 and TGS-2610 sensors are generalist hydrocarbon and contaminant sensors, these sensors were less sensitive to changes in methane than the TGS-2611, which is specific to methane.

V. CONCLUSION

Based on the comparison of these commercially available low-cost sensors, selection of a sensor for practical applications can be simplified. The obvious choice for low concentration applications is the Gascard series of sensors. However, this sensor is comparatively more expensive than the other sensors in this paper on a scale of 10-100 times. For applications with modest budgets, the K-30 and Telaire sensors are viable for carbon dioxide detection, and the TGS-2611 sensor is similarly viable for methane. The K-30 sensor costs roughly a tenth of the cost of the similarly-able Telaire sensor. Therefore, we also recommend it over the Telaire offering. The MQ-4 is an incredibly inexpensive alternative to the TGS series, available for only a few dollars. For very low cost devices, the MQ-4 sensor is an option if the user only needs a rough estimate of concentration, rather than the precision found in other, more expensive, offerings. During our study, the TGS sensors proved difficult to purchase, most suppliers not stocking this device and only at a high price when available. Use of the Dynament sensors is not advisable due to inaccuracies and inconsistencies of the devices considering their cost (roughly 100 times that of the MQ-4 sensor).

Sensor choice for the detection of ppm level concentration of carbon dioxide and methane is a matter of compromises. There appears to be no single sensor which simultaneous fulfills traits of sensitivity at atmospheric levels, low power consumption, low price, and market availability. It is the opinion of the authors that the devices which best fill these needs from the available options are the K-30 and MQ-4 sensor. The K-30 sensor provided acceptable sensitivity for a low cost in terms of money and power. The MQ-4 sensor appears to be very insensitive to small changes in concentration, and data it produces should not taken as accurate. However, the MQ-4 does appear to be able to detect larger changes in concentration which would represent localized leak. We believe that the TGS-2611 would be more suited to this task, but the difficulty in acquisition prevents it from being a viable option at scale at this time.

ACKNOWLEDGMENT

REFERENCES

[1] Z. Yang, N. Li, B. Becerik-Gerber, and M. Orosz, "A systematic approach to occupancy modeling in ambient sensor-rich buildings," *SIMULATION*, vol. 90, no. 8, pp. 960–977, Aug. 2014, bibtex: yang_systematic_2014. [Online]. Available: http://sim.sagepub.com/content/90/8/960.abstract

[2] W.-Y. Chung and S.-C. Lee, "A selective AQS system with artificial neural network in automobile," *Proceedings of the Eleventh International Meeting on Chemical Sensors IMCS-11IMCS 2006IMCS 11*, vol. 130, no. 1, pp. 258–263, Mar. 2008, bibtex: chung_selective_2008. [Online]. Available: http://www.sciencedirect.com/science/article/pii/S0925400507006120

[3] W. Won and K. S. Lee, "Nonlinear observer with adaptive grid allocation for a fixed-bed adsorption process," *Computers & Chemical Engineering*, vol. 46, pp. 69–77, Nov. 2012. [Online]. Available: http://www.sciencedirect.com/science/article/pii/S0098135412002293

[4] P. Yi, L. Xiao, and Y. Zhang, "Remote real-time monitoring system for oil and gas well based on wireless sensor networks," in *Mechanic Automation and Control Engineering (MACE), 2010 International Conference on*, Jun. 2010, pp. 2427–2429, bibtex: yi_remote_2010.

[5] A. Somov, A. Baranov, D. Spirjakin, A. Spirjakin, V. Sleptsov, and R. Passerone, "Deployment and evaluation of a wireless sensor network for methane leak detection," *Selected Papers from the 26th European Conference on Solid-State Transducers Krakw, Poland, 9-12 September 2012*, vol. 202, pp. 217–225, Nov. 2013, bibtex: somov_deployment_2013. [Online]. Available: http://www.sciencedirect.com/science/article/pii/S0924424712007297

[6] T. Pering, G. Tamburello, A. McGonigle, A. Aiuppa, A. Cannata, G. Giudice, and D. Patan, "High time resolution fluctuations in volcanic carbon dioxide degassing from Mount Etna," *Journal of Volcanology and Geothermal Research*, vol. 270, pp. 115–121, Jan. 2014. [Online]. Available: http://dx.doi.org/10.1016/j.jvolgeores.2013.11.014

[7] R. Black, C. (Mick) Meyer, A. Yates, L. V. Zweiten, and J. Mueller, "Formation of artefacts while sampling emissions of PCDD/PCDF from open burning of biomass," *Chemosphere*, vol. 88, no. 3, pp. 352–357, Jul. 2012. [Online]. Available: http://www.sciencedirect.com/science/article/pii/S0045653512003864

[8] H. Guohua, W. Lvye, M. Yanhong, and Z. Lingxia, "Study of grass carp (Ctenopharyngodon idellus) quality predictive model based on electronic nose," *Sensors and Actuators B: Chemical*, vol. 166167, pp. 301–308, May 2012. [Online]. Available: http://www.sciencedirect.com/science/article/pii/S0925400512001992

[9] S. Karunanithi, N. M. Din, H. Hakimie, C. K. Hua, R. C. Omar, and T. C. Yee, "Performance of labscale solar powered wireless landfill monitoring system," in *Energy and Environment, 2009. ICEE 2009. 3rd International Conference on*, Dec. 2009, pp. 443–448, bibtex: karunanithi_performance_2009.

[10] D. G. Shendell, J. H. Therkorn, N. Yamamoto, Q. Meng, S. W. Kelly, and C. A. Foster, "Outdoor near-roadway, community and residential pollen, carbon dioxide and particulate matter measurements in the urban core of an agricultural region in central CA," *Atmospheric Environment*, vol. 50, pp. 103–111, Apr. 2012. [Online]. Available: http://www.sciencedirect.com/science/article/pii/S135223101101346X

[11] S.-W. Chiu and K.-T. Tang, "Towards a Chemiresistive Sensor-Integrated Electronic Nose: A Review," *Sensors*, vol. 13, no. 10, pp. 14 214–14 247, Oct. 2013. [Online]. Available: http://dx.doi.org/10.3390/s131014214

[12] C. K. Ho, M. T. Itamura, M. Kelley, and R. C. Hughes, "Review of Chemical Sensors for Real-Time In-Situ Sensing," Sandia National Laboratories, Tech. Rep. SAND2001-0643, 2001. [Online]. Available: http://www.sandia.gov/sensor/SAND2001-0643.pdf

[13] T. Blasing, "Recent Greenhouse Gas Concentrations," U. S. Department of Energy, CDIAC, Tech. Rep., 2016. [Online]. Available: http://cdiac.ornl.gov/pns/current_ghg.html

[14] E. Dlugokencky and P. Tans, "Trends in Atmospheric Carbon Dioxide," NOAA/ESRL, Tech. Rep., 2016. [Online]. Available: www.esrl.noaa.gov/gmd/ccgg/trends

[15] A. J. Turner, D. J. Jacob, J. Benmergui, S. C. Wofsy, J. D. Maasakkers, A. Butz, O. Hasekamp, and S. C. Biraud, "A large increase in U.S. methane emissions over the past decade inferred from satellite data and surface observations," *Geophysical Research Letters*, vol. 43, no. 5, pp. 2218–2224, Mar. 2016. [Online]. Available: http://dx.doi.org/10.1002/2016GL067987

[16] I. Bamberger, J. Stieger, N. Buchmann, and W. Eugster, "Spatial variability of methane: Attributing atmospheric concentrations to emissions," *Environmental Pollution*, vol. 190, pp. 65–74, Jul. 2014. [Online]. Available: http://www.sciencedirect.com/science/article/pii/S0269749114001195

[17] E. Dlugokencky, "Trends in Atmospheric Methane," NOAA/ESRL, Tech. Rep., 2016. [Online]. Available: www.esrl.noaa.gov/gmd/ccgg/trends_ch4

[18] G. Neri, "First Fifty Years of Chemoresistive Gas Sensors," *Chemosensors*, vol. 3, no. 1, pp. 1–20, Jan. 2015. [Online]. Available: http://dx.doi.org/10.3390/chemosensors3010001

[19] R. Frodl and T. Tille, "A High-Precision NDIR Gas Sensor for Automotive Applications," *IEEE Sensors Journal*, vol. 6, no. 6, pp. 1697–1705, Dec. 2006.

[20] Z. Zhu, Y. Xu, and B. Jiang, "A One ppm NDIR Methane Gas Sensor with Single Frequency Filter Denoising Algorithm," *Sensors (Basel, Switzerland)*, vol. 12, no. 9, pp. 12 729–12 740, 2012. [Online]. Available: http://www.ncbi.nlm.nih.gov/pmc/articles/PMC3478867/

[21] Z. Bacsik, J. Mink, and G. Keresztury, "FTIR Spectroscopy of the Atmosphere. I. Principles and Methods," *Applied Spectroscopy Reviews*, vol. 39, no. 3, pp. 295–363, Dec. 2004. [Online]. Available: http://dx.doi.org/10.1081/ASR-200030192

[22] Coblentz Society, Inc., "Evaluated Infrared Reference Spectra," in *NIST Chemistry WebBook*, ser. NIST Standard Reference Database, P. J. Lindstrom and W. G. Mallard, Eds. Gaithersburg MD, 20899: National Institute of Standards and Technology, no. 69. [Online]. Available: http://webbook.nist.gov

[23] L. Wang and R. Kumar, "Thick film CO2 sensors based on Nasicon solid electrolyte," *Solid State Ionics*, vol. 158, no. 34, pp. 309–315, Mar. 2003. [Online]. Available: http://www.sciencedirect.com/science/article/pii/S0167273802008408

[24] K. J. Albert, N. S. Lewis, C. L. Schauer, G. A. Sotzing, S. E. Stitzel, T. P. Vaid, and D. R. Walt, "Cross-Reactive Chemical Sensor Arrays," *Chemical Reviews*, vol. 100, no. 7, pp. 2595–2626, Jul. 2000. [Online]. Available: http://dx.doi.org/10.1021/cr980102w

[25] C. Wang, L. Yin, L. Zhang, D. Xiang, and R. Gao, "Metal oxide gas sensors: sensitivity and influencing factors," *Sensors*, vol. 10, no. 3, pp. 2088–2106, 2010.

[26] M. Prudenziati and B. Morten, "Thick-film sensors: an overview," *Sensors and Actuators*, vol. 10, no. 1, pp. 65–82, Sep. 1986. [Online]. Available: http://www.sciencedirect.com/science/article/pii/025068748680035X

[27] C. Di Natale, F. Davide, G. Faglia, and P. Nelli, "Study of the effect of the sensor operating temperature on SnO2-based sensor-array performance," *The workshop on new developments in semiconducting gas sensors*, vol. 23, no. 2, pp. 187–191, Feb. 1995. [Online]. Available: http://www.sciencedirect.com/science/article/pii/092540059401274L

[28] W. Eugster and G. W. Kling, "Performance of a low-cost methane sensor for ambient concentration measurements in preliminary studies." *Atmospheric Measurement Techniques*, vol. 5, no. Copyright (C) 2015 American Chemical Society (ACS). All Rights Reserved., pp. 1925–1934, 2012.

[29] Janusz Marek Smulko, Maciej Trawka, Claes Goran Granqvist, Radu Ionescu, Fatima Annanouch, Eduard Llobet, and Laszlo Bela Kish, "New approaches for improving selectivity and sensitivity of resistive gas sensors: a review," *Sensor Review*, vol. 35, no. 4, pp. 340–347, Sep. 2015. [Online]. Available: http://dx.doi.org/10.1108/SR-12-2014-0747

[30] L. H. Keith, W. Crummett, J. Deegan, R. A. Libby, J. K. Taylor, and G. Wentler, "Principles of environmental analysis," *Analytical Chemistry*, vol. 55, no. 14, pp. 2210–2218, 1983. [Online]. Available: http://dx.doi.org/10.1021/ac00264a003

[31] Mocak J., Bond A. M., Mitchell S., and Scollary G., "A statistical overview of standard (IUPAC and ACS) and new procedures for determining the limits of detection and quantification: Application to voltammetric and stripping techniques (Technical Report)," *Pure and Applied Chemistry*, vol. 69, no. 2, p. 297, 2009. [Online]. Available: //www.degruyter.com/view/j/pac.1997.69.issue-2/pac199769020297/pac199769020297.xml

[32] N. Barsan, M. Schweizer-Berberich, and W. Gpel, "Fundamental and practical aspects in the design of nanoscaled SnO2 gas sensors: a status report," *Fresenius' Journal of Analytical Chemistry*, vol. 365, no. 4, pp. 287–304, 1999. [Online]. Available: http://dx.doi.org/10.1007/s002160051490

[33] S. Ahlers, G. Mller, and T. Doll, "A rate equation approach to the gas sensitivity of thin film metal oxide materials," *Sensors and Actuators B: Chemical*, vol. 107, no. 2, pp. 587–599, Jun. 2005. [Online]. Available: http://www.sciencedirect.com/science/article/pii/S0925400504007580

[34] T. Williams and C. Kelley, "gnuplot 5.0: An Interactive Plotting Program," Jan. 2016. [Online]. Available: http://www.gnuplot.info/docs_5.0/gnuplot.pdf